JOURNAL OF COMPUTATIONAL PHYSICS **138,** 331–353 (1997)
ARTICLE NO. CP975822

Unfolding Sphere Size Distributions with a Density Estimator Based on Tikhonov Regularization

J. Weese,*[,1] E. Korat,* D. Maier,* and J. Honerkamp*[,†]

**Freiburger Materialforschungszentrum, Stefan-Meier-Strasse 21, D-79104 Freiburg im Breisgau, Germany; †Albert-Ludwigs-Universität Freiburg, Fakultät für Physik, Hermann-Herder-Strasse 3, D-79104 Freiburg im Breisgau, Germany*
E-mail: hon@phyq1.physik.uni-freiburg.de

Received October 15, 1996; revised June 17, 1997

In a large number of measuring and characterization methods, the sphere size distribution of particles embedded in a medium has to be estimated from profile radii observed in cross sections or thin slices. On the one hand, this is a typical problem of density estimation. For that reason, kernel estimators may be applied. On the other hand, the computation of the sphere size distribution from the profile size distribution requires the inversion of an integral equation. In the case of cross sections or infinitely thin slices, this is an ill-posed problem which can be solved with specific methods as, e.g., Tikhonov regularization. In this contribution we propose a method for unfolding the sphere size distribution given a sample of profile radii which combines the advantages of kernel estimators with those of regularization methods. In order to study and test this method, Monte-Carlo simulations have been performed. The results demonstrate that the method is reliable and leads to properly unfolded sphere size distributions. Finally, the method has been applied to experimental data obtained from transmission electron microscopy images of several polymer blends. The results demonstrate that the new method is a valuable tool for data analysis.

Key Words: stereology; sphere size distribution; profile radii; density estimation; ill-posed problem; Tikhonov regularization; polymer blend; transmission electron microscopy.

[1] Present address: Philips Research Research Division Technical Systems Hamburg, P.O. Box 63 05 65, D-22315 Hamburg, Germany.

0021-9991/97 $25.00

1. INTRODUCTION

There is a large number of measuring and characterization methods in very different disciplines as, e.g. physics, chemistry, metallurgy, biology, geology, and medicine, where the sphere size distribution of particles embedded in a medium has to be estimated. Often, the spherical particles cannot be observed directly and circular profiles obtained by taking cross sections through the sample or by preparing thin slices of the sample are studied in order to get information about the sphere size distribution. Obviously, the radii of the profiles are smaller than the radii of the corresponding spheres. Therefore, the problem of unfolding the sphere size distribution given a sample of profile radii—a problem well-known as Wicksell's corpuscle problem [1]—arises. This problem can be avoided if it is possible to use the information of two parallel planes with known distance, a so called disector. In this case the problem is fully determined and it is not necessary to solve Wicksell's problem [2, 3], but this technique cannot be applied in any case.

A specific problem where the unfolding of sphere size distributions is of interest, concerns blends of two immiscible thermoplastics. Many of these materials have a morphology with one component building a matrix in which approximately spherical particles of the other component are randomly dispersed. The particle radii range from about 50 nm up to several μm, and the morphology of such blends can be characterized by studying thin slices of 50–200 nm thickness with transmission electron microscopy (TEM). In that way, several thousand profile radii can be measured. These profiles can be used to unfold the sphere size distribution making it possible to relate this quantity to the conditions during preparation of the blend or the rheological properties of its melt [4–11].

The estimation of the sphere size distribution from a sample of profile radii may be considered as a combination of two problems. On the one hand, it is a typical problem of density estimation for which usually kernel estimators [12] are used. The application of kernel estimators has been proposed and discussed in [13–15]. This approach looks promising, but there remain some open questions: the result obtained by a kernel estimator depends on the width of the kernel. This parameter controls the smoothness of the result and has essentially the same meaning as the bandwidth of a filter for smoothing noisy data. There is, however, no method for the optimal estimation of this parameter available and it must be adjusted manually. Furthermore, the result for the sphere size distribution may have negative values and it is not properly normalized.

On the other hand, in the case of cross sections or infinitely thin slices the determination of the sphere size distribution from the profile size distribution requires the inversion of an integral equation of the first kind. This is an ill-posed problem (see [16] for a definition of ill-posed problems) with the consequence that the condition number of a set of linear equations approximating this integral equation becomes worse if the number of discrete points is increased [17]. In order to avoid the resulting instability, regularization methods [18] should be used. The determination of the sphere size distribution by calculation of a histogram of the profile radii and subsequent application of Tikhonov regularization has been proposed and discussed in [19, 20]. There is a parameter controlling the smoothness

of the result but in contrast to the work about kernel estimators, methods for the optimal estimation of this parameter have been applied. In addition, it was shown in [20] that positivity constraints can be taken into account in such a way that the result for the sphere size distribution does not have negative values. Nevertheless, there are some problems due to the histogram of the profile radii: the result for the sphere size distribution depends slightly on the number and the distribution of the histogram's bins. In addition, the statistical properties of the histogram can only approximately be taken into account. Difficulties arise especially in the case of a considerable number of empty bins.

In this contribution we propose a method for unfolding sphere size distributions given a sample of profile radii which combines the advantages of the kernel estimators with those of the regularization methods; on the one hand, it is shown in what way a nonnegative and properly normalized result for the sphere size distribution can be defined. Furthermore, a method to estimate the optimal degree of smoothness is presented. On the other hand, the method does not require the construction of a histogram from the profile radii. The method has been studied using simulated data. In addition, it has been applied to experimental data obtained from TEM images of several polymer blends.

In the following section the well-known integral equation relating the profile size distribution to the corresponding sphere size distribution is presented. The method for unfolding sphere size distributions is described in Section 3. Section 4 includes the results of the study based on simulations. The experiences and results with experimental data are summarized in Section 5. Details about the numerical computations in connection with the unfolding are outlined in the Appendix.

2. RELATION BETWEEN THE PROFILE AND THE SPHERE SIZE DISTRIBUTION

When unfolding the sphere size distribution $q(R)$ given a sample $r_1, ..., r_n$ of profile radii, the relation between this distribution and the profile size distribution $p(r)$ must be known. This relation depends on the thickness d of the slices under investigation. In addition it must be kept in mind that profiles with radii below some resolution limit ε can usually not be resolved. A consequence of this resolution limit is that the sphere size distribution $q(R)$ can only be unfolded for radii $R \geq \varepsilon$.

The relation between both distributions has been studied and discussed in detail (see, e.g., [19, 21–23]). Assuming

- that the particles are distributed randomly and homogeneously,
- that the particles are opaque,
- that overlapping particles can be neglected, and
- that effects due to the rim of the slice can be neglected,

the equation

$$p(r) = \frac{d}{d + 2\overline{R}}\, q(r) + \frac{2}{d + 2\overline{R}} \int_r^{R_{\max}} \frac{r}{\sqrt{R^2 - r^2}}\, q(R)\, dR, \quad \varepsilon \leq r \leq R_{\max}, \tag{1}$$

can be derived. In this equation, $R_{\max}$ denotes an upper limit of the sphere radius and

$$\overline{R} = \int_{\varepsilon}^{R_{\max}} \sqrt{R^2 - \varepsilon^2}\, q(R)\, dR \tag{2}$$

is a normalization factor, so that

$$\int_{\varepsilon}^{R_{\max}} p(r)\, dr = 1 \tag{3}$$

holds. The first term in Eq. (1) is caused by spheres with centers inside the slice. For these spheres the true radii are obtained. The second term is due to spheres cut by the slice, but with centers outside the slice. For these spheres, radii smaller than the true radii are measured. It should be mentioned that Eq. (1) is an Abel integral equation of the first kind for infinitely thin slices ($d = 0$) and else it is an Abel integral equation of the second kind. In the former case the ill posedness of the sphere size distribution problem corresponds to a half-differentiation [24]. Furthermore, it should be mentioned that the more general relations, including overprojection, capping angles, and resolution threshold, can be found in [25].

For the unfolding method introduced in the following section, the relation between the cumulative sphere size distribution function

$$P(r) = \int_{\varepsilon}^{r} p(r')\, dr' \tag{4}$$

and the scaled sphere size distribution

$$h(R) = \frac{1}{d + 2\overline{R}}\, q(R) \tag{5}$$

is needed. Taking the normalization of $q(R)$

$$\int_{\varepsilon}^{R_{\max}} q(R)\, dR = 1 \tag{6}$$

into account, integration of Eq. (1) leads to

$$P(r) = 1 - 2\int_{r}^{R_{\max}} \left(\frac{d}{2} + \sqrt{R^2 - r^2}\right) h(R)\, dR. \tag{7}$$

Defining the integral operator K according to

$$(Kh)(r) = 2\int_{r}^{R_{\max}} \left(\frac{d}{2} + \sqrt{R^2 - r^2}\right) h(R)\, dR \quad \text{for } \varepsilon \le r \le R_{\max} \tag{8}$$

and the function $I(r)$ by

$$I(r) = 1, \quad \varepsilon \le r \le R_{\max}, \tag{9}$$

this integral equation can be written as

$$(Kh) = I - P. \tag{10}$$

3. A METHOD FOR UNFOLDING THE SPHERE SIZE DISTRIBUTION

In the first part of this section, the result for the sphere size distribution is defined using Tikhonov regularization for a given value of the so-called regularization parameter. As indicated in the Introduction, this parameter controls the degree of smoothness of the result, and it has a strong influence on the unfolded sphere size distribution. For that reason a procedure to estimate an appropriate value of this parameter is presented in the second part of this section. In the last part, intervals characterizing the statistical variance of the unfolded sphere size distribution are introduced.

3.1. *Density Estimation by Tikhonov Regularization*

The starting point of the unfolding method based on Tikhonov regularization is the empirical cumulative distribution function $\hat{P}(r)$ of the sample $r_1, ..., r_n$ of profile radii. The empirical cumulative distribution function is a consistent estimate of the cumulative distribution function $P(r)$ and can be written as

$$\hat{P}(r) = \frac{1}{n} \sum_{i=1}^{n} \theta_{r_i}(r) \tag{11}$$

with

$$\theta_a(r) = \begin{cases} 0, & r < a, \\ 1, & r \geq a. \end{cases} \tag{12}$$

Using Tikhonov regularization, an estimate $\hat{h}_\lambda$ of the scaled sphere size distribution h can be defined by the minimum of

$$V(\lambda) = \|\hat{P} - (I - (Kh))\|^2 + \lambda \|Lh\|^2 \tag{13}$$

with respect to h. Alternatively, the estimate $\hat{h}_\lambda$ can be written as

$$\hat{h}_\lambda = K^{-1}(\lambda)(I - \hat{P}) \tag{14}$$

with

$$K^{-1}(\lambda) = (K^t K + \lambda L^t L)^{-1} K^t. \tag{15}$$

In these equations L denotes the second derivative, the norm $\|\cdot\|$ of an arbitrary function f is given by

$$\|f\|^2 = \int_{\varepsilon}^{R_{\max}} f^2(s)\, ds, \tag{16}$$

and λ denotes the regularization parameter. With an appropriate value of this parameter, the first term on the right-hand side of Eq. (13) forces the result to be compatible with the data. The second term leads to a smooth estimate $\hat{h}_\lambda$ of the

scaled sphere size distribution h. An estimate of $\hat{q}_\lambda$ of the sphere size distribution q itself can be obtained by normalization:

$$\hat{q}_\lambda(R) = \frac{\hat{h}_\lambda(R)}{\int_\varepsilon^{R_{\max}} \hat{h}_\lambda(R')\, dR'}. \tag{17}$$

So far it has not been taken into account that the scaled sphere size distribution h is nonnegative. In addition, Eqs. (1) and (5) imply normalization according to

$$2 \int_\varepsilon^{R_{\max}} \left(\frac{d}{2} + \sqrt{R^2 - \varepsilon^2} \right) h(R)\, dR = 1. \tag{18}$$

An estimate satisfying these constraints can be obtained by restricting minimization of the functional $V(\lambda)$ to nonnegative and properly normalized functions. In this case, $\hat{h}_\lambda$ can no longer be written in a form similar to Eq. (14).

3.2. *Optimal Estimation of the Regularization Parameter*

It is obvious that the quality of the estimate $\hat{h}_\lambda$ depends strongly on the regularization parameter λ which has essentially the same influence on the result as the bandwidth of a filter for smoothing noisy data. If this parameter is too small, the result will show oscillations. On the other hand, the result will be oversmoothed if this parameter is too large. Thus, a good and reliable procedure for the estimation of the regularization parameter is necessary.

The procedure for the estimation of the regularization parameter described in this contribution is based on the principle of the SC-method (SC for self-consistent). This method has been proposed in [26] and led to better results than other well-known procedures for this purpose. In addition, the SC-method has successfully been applied to solve various linear as well as nonlinear ill-posed problems [4, 20, 27–32]. Other possible methods to estimate a value of the regularization parameter are the cross-validation method and the discrepancy method [33].

In order to introduce the SC-method, the error

$$d_h = \|h - \hat{h}_\lambda\|^2 \tag{19}$$

of the estimate $\hat{h}_\lambda$ is considered. This error is a realization of a random variable denoted by D_h. The expectation value,

$$ED_h = ED_h(h, \lambda, n), \tag{20}$$

of this random variable depends on the scaled sphere size distribution h, the regularization parameter λ, and the number of profile radii n. A good value of the regularization parameter should minimize this quantity:

$$\frac{\partial}{\partial \mu} ED_h(h, \mu, n) \big|_{\mu=\lambda} = 0. \tag{21}$$

Actually, this equation cannot be solved in practice, because the scaled sphere size distribution h is not known.

The idea of the SC-method is to replace the scaled sphere size distribution h in Eq. (21) by the best estimate which can be obtained from the data. The distribution h is, therefore, replaced by $\hat{h}_\lambda$ leading to the equation

$$\frac{\partial}{\partial \mu} ED_h(\hat{h}_\lambda, \mu, n) \,|_{\mu=\lambda} = 0. \tag{22}$$

This equation defines a value λ_{SC} for the regularization parameter. If this value leads to a good estimate $\hat{h}_\lambda$, the replacement of the distribution h by the estimate $\hat{h}_\lambda$ is justified and Eq. (22) should define a good value for the regularization parameter. By solving Eq. (22) the regularization parameter has therefore been estimated in a self-consistent manner.

In principle, the quantity $ED_h(h, \lambda, n)$ can be evaluated by a Monte-Carlo procedure. This is, however, very time consuming, and an explicit expression of the quantity $ED_h(h, \lambda, n)$ should be known in order to apply the SC-method in practice. If the positivity constraints are taken into account, such an explicit expression can hardly be derived. Because of these constraints it is even impossible to obtain a more explicit formula of the estimate $\hat{h}_\lambda$ defined by the minimum of $V(\lambda)$. On the other hand, it will be shown in Section 4 that the positivity constraints do not have a crucial influence on the optimal regularization parameter. For that reason the SC-method can be applied without taking the constraints into account. In this case, the estimate $\hat{h}_\lambda$ is given by Eq. (14). Using this relation as well as Eqs. (4), (10), and (11) the expression

$$\begin{aligned} ED_h(h, \lambda, n) = {} & \|h - K^{-1}(\lambda)(I - Kh)\|^2 \\ & + \frac{1}{n} \int_\varepsilon^{R_{\max}} \|K^{-1}(\lambda)\theta_r\|^2 \, |(Kh)'(r)| \, dr \\ & - \frac{1}{n} \|K^{-1}(\lambda)(I - Kh)\|^2 \end{aligned} \tag{23}$$

can be derived by a straightforward calculation. The first term on the right-hand side of this equation is due to the estimator's bias, whereas the second and the third terms are a consequence of the variance.

3.3. *Statistical Variance of the Estimate*

Whenever a quantity is estimated, it is desirable to obtain, in addition to the estimate itself, information about its statistical variation. For that reason, confidence intervals should be calculated. These intervals are usually defined in such a way that the true value of the quantity is in the interval with a probability of 68%. In many statistical contexts confidence levels of 95% or more are chosen.

An estimate obtained by regularization is affected by two errors, one being a bias caused by regularization and the other one being a statistical error due to the statistical properties of the data. In the case of an ill-posed problem, the bias cannot

be estimated and confidence intervals can, therefore, not be defined. Despite this fact, error intervals describing the influence of the statistical properties of the data are useful for the interpretation of the result. Denoting the variance of the random variable corresponding to $\hat{h}_\lambda(R)$ by $\sigma^2(R)$, such intervals can be defined by

$$\begin{aligned} &[\hat{h}_\lambda(R) - \sigma(R), \hat{h}_\lambda(R) + \sigma(R)] \quad \text{for } \hat{h}_\lambda(R) - \sigma(R) \geq 0 \\ &[0, \hat{h}_\lambda(R) + \sigma(R)] \quad \text{for } \hat{h}_\lambda(R) - \sigma(R) < 0. \end{aligned} \tag{24}$$

Normalization according to Eq. (17) leads to error intervals for the estimate $\hat{q}_\lambda(R)$ of the sphere size distribution.

To estimate these error intervals, the variances $\sigma^2(R)$ must be evaluated. If the constraints are neglected, Eqs. (4), (10), (11), and (14) can be used to derive an explicit expression for the variances,

$$\begin{aligned} \sigma^2(R) = &\frac{1}{n} \int_\varepsilon^{R_{\max}} ((K^{-1}(\lambda)\theta_r)(R))^2 \, |(Kh)'(r)| \, dr \\ &- \frac{1}{n} (K^{-1}(\lambda)(I - Kh)(R))^2, \end{aligned} \tag{25}$$

which can approximately be evaluated if the true scaled sphere size distribution $h(R)$ is replaced by the estimate $\hat{h}_\lambda(R)$. Compared to the estimation of the regularization parameter with the SC-method and the evaluation of the quantity $ED_h(h, \lambda, n)$, the positivity constraints can, however, not be simply neglected, because they have a considerable influence on the estimate $\hat{h}_\lambda(R)$. For that reason it is necessary to account for the positivity constraints and a method to do this, without performing a time-consuming Monte Carlo simulation, is included in the Appendix in which the numerical computations are described.

4. RESULTS FOR SIMULATED DATA

In order to study and test the unfolding method presented in the preceding section, Monte-Carlo simulations have been performed. First, a sphere size distribution was chosen and the corresponding profile size distribution was computed by numerical integration according to Eq. (1). For that profile size distribution 200 samples with n radii each were generated. For each sample the estimate $\hat{h}_\lambda$ and the corresponding error d_h were calculated in dependence on the regularization parameter λ which was varied from $\lambda = 10^{-15}$ up to $\lambda = 10^{-2}$. This was done twice: on the one hand, positivity constraints and normalization were taken into account and, on the other hand, these constraints were neglected. By averaging the values of d_h over the 200 samples, the expected error $ED_h(h, \lambda, n)$ in dependence on the regularization parameter λ was obtained for the case that constraints are taken into account, as well as for the case that they are neglected. In addition, the regularization parameter defined by the SC-method was estimated for each sample.

Such Monte-Carlo simulations have been performed for a unimodal and for a bimodal sphere size distribution using 200 samples with n = 1000, 2000, and 5000

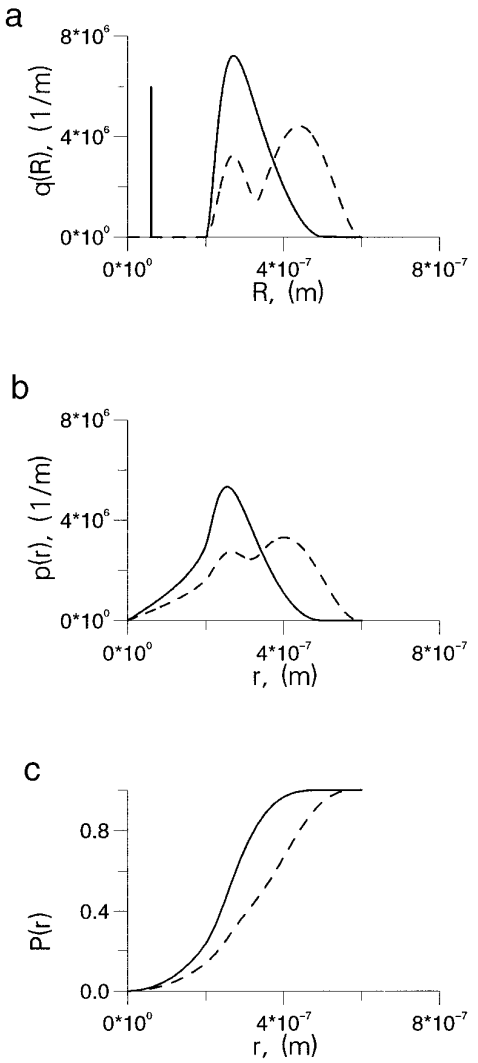

FIG. 1. Unimodal (solid line) and bimodal (dashed line) sphere size distribution used to test the unfolding method (a). The corresponding profile size distributions, (b) and the cumulative profile size distribution functions, (c) are also shown. The straight line in (a) marks the thickness d of the slices.

profile radii. Figure 1 shows both sphere size distributions, together with the corresponding profile size distributions and the cumulative profile size distribution functions. The two sphere size distributions were calculated according to

$$q(R) = \begin{cases} \sum_{j=1}^{2} h_j\{(R_{min}(j) - R)^2(R_{max}(j) - R)^2\} & for\ R \in [R_{\min}(j), R_{\max}(j)] \\ 0, & else. \end{cases} \tag{26}$$

The parameters are listed in Table I. The order of magnitude of the spheres, as well as the slice thickness (d = 60 nm), have been chosen to be typical for TEM

TABLE I
Parameters of the Unimodal and the Bimodal Sphere Size Distribution

Parameter	Unimodal distribution	Bimodal distribution
$R_{min}(1)$	$7 \times 10^{-8}\ m$	$9 \times 10^{-8}\ m$
$R_{min}(2)$	$16 \times 10^{-8}\ m$	$15 \times 10^{-8}\ m$
$R_{max}(1)$	$27 \times 10^{-8}\ m$	$29 \times 10^{-8}\ m$
$R_{max}(2)$	$44 \times 10^{-8}\ m$	$35 \times 10^{-8}\ m$
h_1	20.0	20.0
h_2	1.0	1.0

images of immiscible polymer blends. The results of the Monte-Carlo simulation, i.e. the expected error $ED_h(h, \lambda, n)$ in dependence on the regularization parameter λ and a histogram of the regularization parameter estimated with the SC-method, are shown in Fig. 2 for the unimodal and in Fig. 3 for the bimodal sphere size distribution. In addition, Figs. 4 and 5 show typical results for both distributions if they are unfolded from samples with n = 1000, 2000, and 5000 profile radii.

Figures 2 and 3 show that the expected error $ED_h(h, \lambda, n)$ has a minimum which is at values about $\lambda \approx 10^{-10}$ for the examples presented. If the regularization parameter is increased, the bias introduced by the regularization becomes larger and the expected error $ED_h(h, \lambda, n)$ increases until it reaches an upper bound. If the regularization parameter is decreased, the expected error $ED_h(h, \lambda, n)$ increases because the statistical error becomes larger. In principle, the statistical error becomes arbitrarily large for a vanishing value of the regularization parameter, since the inversion of Eq. (10) is an ill-posed problem. In practical computations, the expected error $ED_h(h, \lambda, n)$ is, however, bounded because of numerical approximations and discretization effects.

The behaviour of the expected error $ED_h(h, \lambda, n)$ for the case that constraints are taken into account is essentially the same as for the case that the constraints are neglected. Except for very large values of the regularization parameter, the constraints lead to a reduction of the expected error $ED_h(h, \lambda, n)$. They have, however, nearly no influence on the regularization parameter λ at which the minimum of the expected error $ED_h(h, \lambda, n)$ is located. Within the estimation of the optimal regularization parameter the constraints can, therefore, be neglected.

The values of the regularization parameter estimated with the SC-method differ about two orders of magnitude within each simulation. Nevertheless, all values are around the minimum of the expected error $ED_h(h, \lambda, n)$ and there was no sample where the estimation of the regularization parameter with the SC-method led to an unacceptable result. A comparison of the regularization parameters obtained for different Monte-Carlo simulations shows that they become smaller if more profiles are used for unfolding the sphere size distribution. This is in agreement with the observation that the value of the expected error $ED_h(h, \lambda, n)$ in the minimum decreases and the minimum moves toward smaller regularization parameters in this case. The unfolded sphere size distributions become, therefore, more accurate.

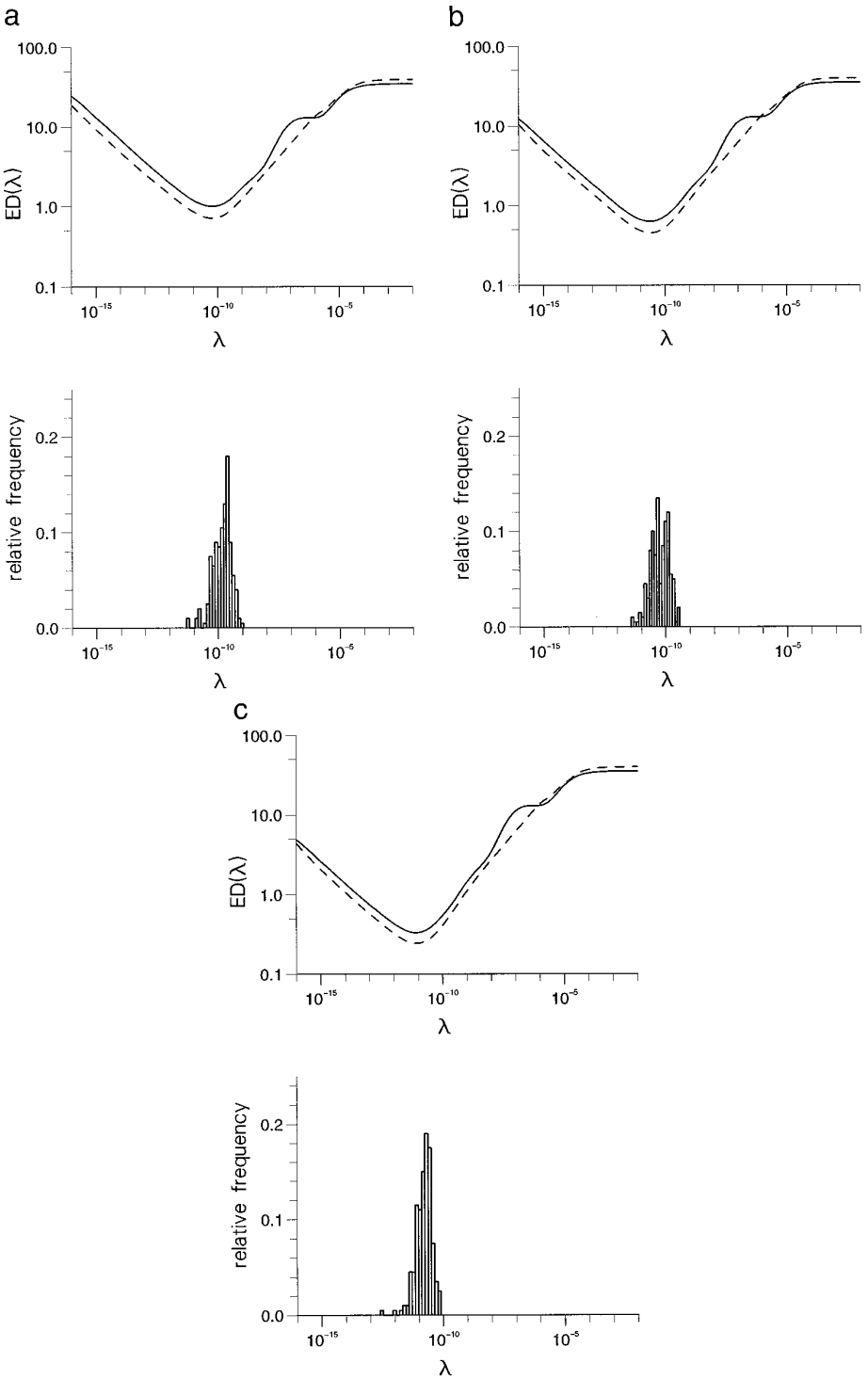

FIG. 2. Expected error of the unimodal sphere size distribution obtained from 1000 (a), 2000 (b), and 5000 (c) profile radii, together with a histogram of the regularization parameters estimated with the SC-method. The expected error $ED_h(h, \lambda, n)$ has been computed for the case that the constraints are neglected (solid line) as well as for the case that they are taken into account (dashed line).

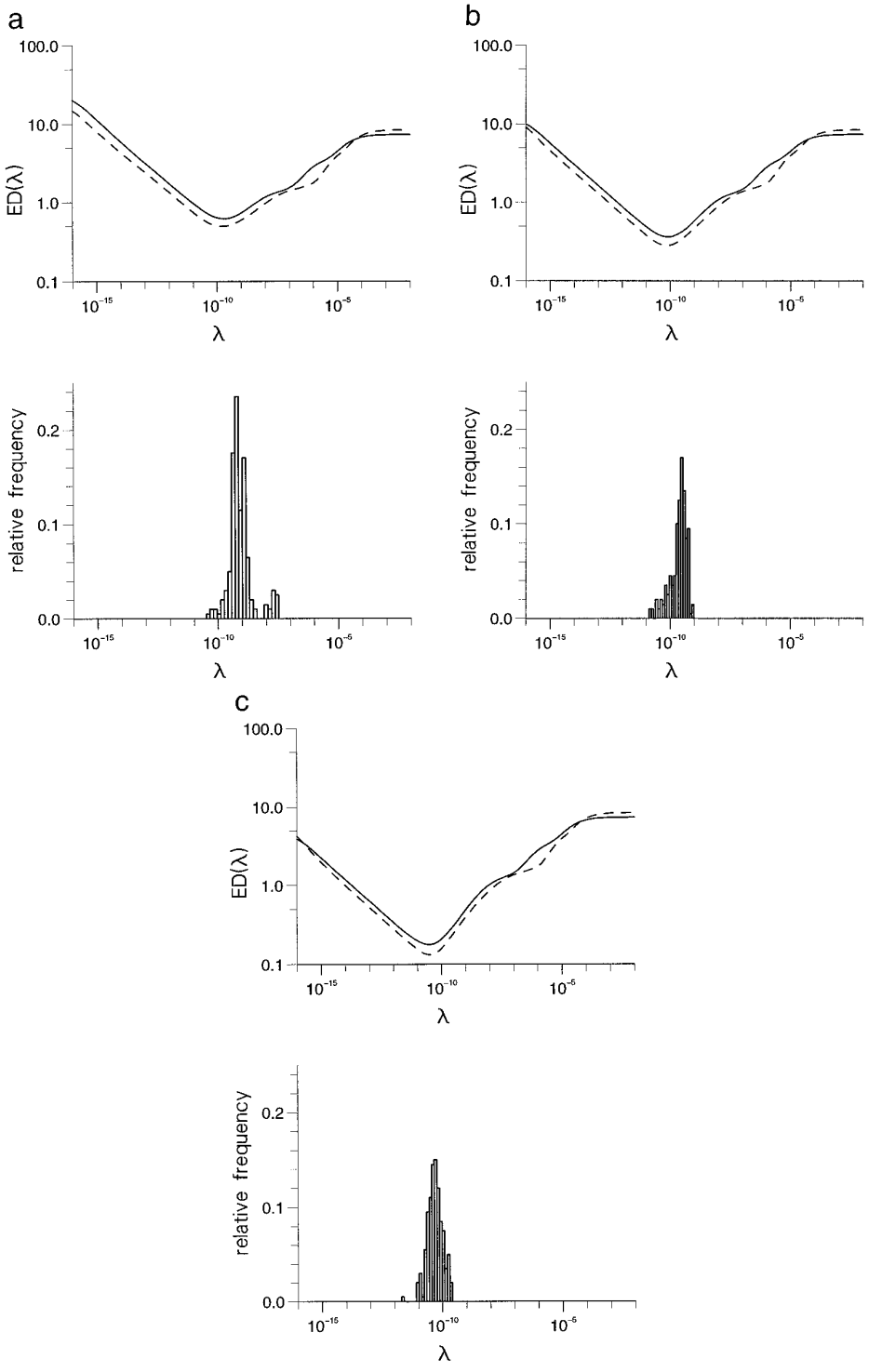

FIG. 3. Expected error of the bimodal sphere size distribution obtained from 1000 (a), 2000 (b), and 5000 (c) profile radii, together with a histogram of the regularization parameters estimated with the SC-method. The expected error $ED_h(h, \lambda, n)$ has been computed for the case that the constraints are neglected (solid line) as well as for the case that they are taken into account (dashed line).

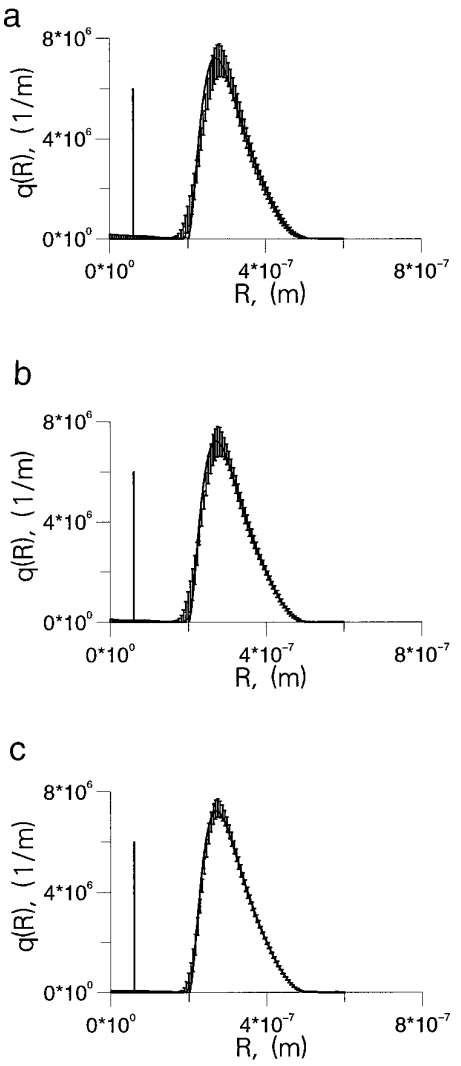

FIG. 4. Typical result for the unimodal sphere size distribution when using 1000 (a), 2000 (b), and 5000 (c) profile radii. The straight line marks the thickness d of the slices.

Figures 4 and 5 confirm that the unfolded sphere size distributions become more accurate if the number of profile radii is increased. To obtain a satisfying result for the unimodal sphere size distribution, 1000 profile radii are sufficient. In contrast to this, the small peak of the bimodal sphere size distribution can only roughly be unfolded with 1000 profiles. However, a good result is obtained with 5000 profiles.

5. APPLICATION TO EXPERIMENTAL DATA

The experimental data have been obtained from a series of polymer blends. They consist of 92.5% polymethylmethacrylate and 7.5% polystyrene with the former

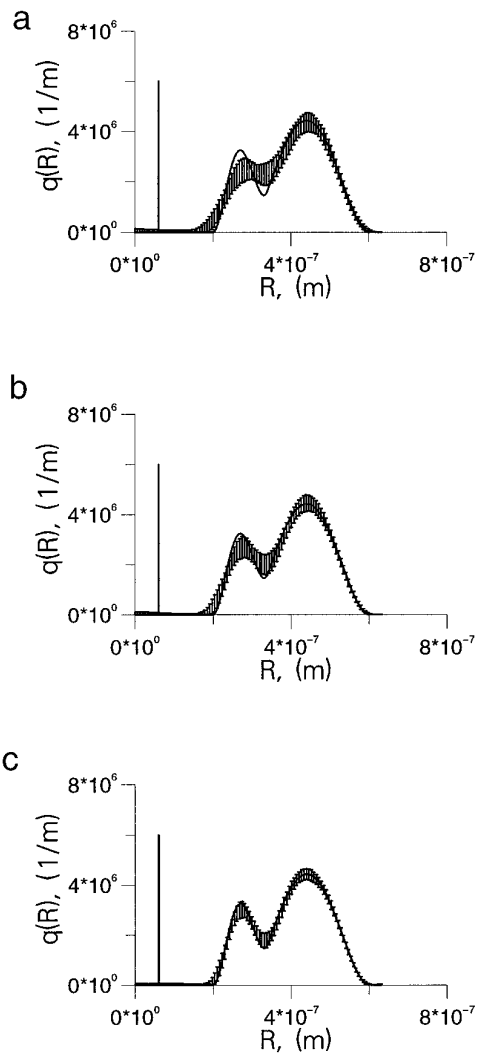

FIG. 5. Typical result for the bimodal sphere size distribution when using 1000 (a), 2000 (b), and 5000 (c) profile radii. The straight line marks the thickness d of the slices.

component being the matrix and the latter one building the inclusions. Except for one blend abbreviated by B075, the blends have been made compatible with the block copolymer poly(cyclohexylmethacrylate-b-methylmethacrylate). The percentage amount of block copolymer added was 5%, 10%, 15%, and 20%, and accordingly, the compatibilized blends are denoted by B075CM05, B075CM10, B075CM15, and B075CM20, respectively. As one part of the block copolymer is compatible with the matrix and the other one with the inclusions, it is deposited at the interface between both blend components affecting the size of the inclusions.

In order to characterize the morphology of the blends, thin slices of 60 nm thickness were prepared and TEM images were taken. A typical example for the uncompatibilized blend B075 is shown in Fig. 6. The radii of the profiles in the

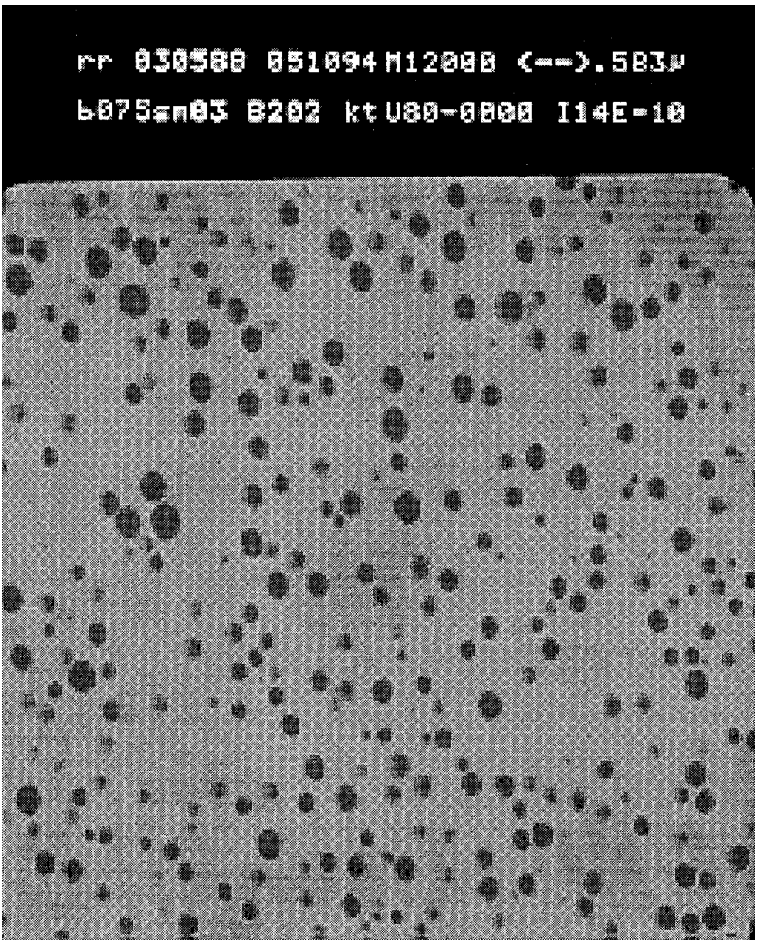

FIG. 6. TEM image of the uncompatibilized blend B075.

TEM images were determined using a commercial image processing software. In that way 2000 up to 4000 profile radii were measured for each blend. As the resolution limit depends on several settings of the microscope, as well as on some parameters of the image processing software, a different value was used for each blend. This value was chosen slightly larger than the smallest profile radii and all profile radii below this limit were discarded. Figure 7 shows the empirical cumulative profile size distribution function and Figure 8 shows the sphere size distributions unfolded with the method presented in Section 3. The number of profiles and the resolution limit used in the computations are summarized in Table II. This table also contains the values obtained for the regularization parameter.

For all samples a unimodal sphere size distribution was obtained. A comparison of the sphere size distribution shows that the size of the inclusions becomes smaller by addition of the block copolymer. For the sample B075 the maximum is at 80 nm, whereas it is only about 40 nm for the sample B075CM20. The width of the sphere size distribution is also affected by the block copolymer and decreases

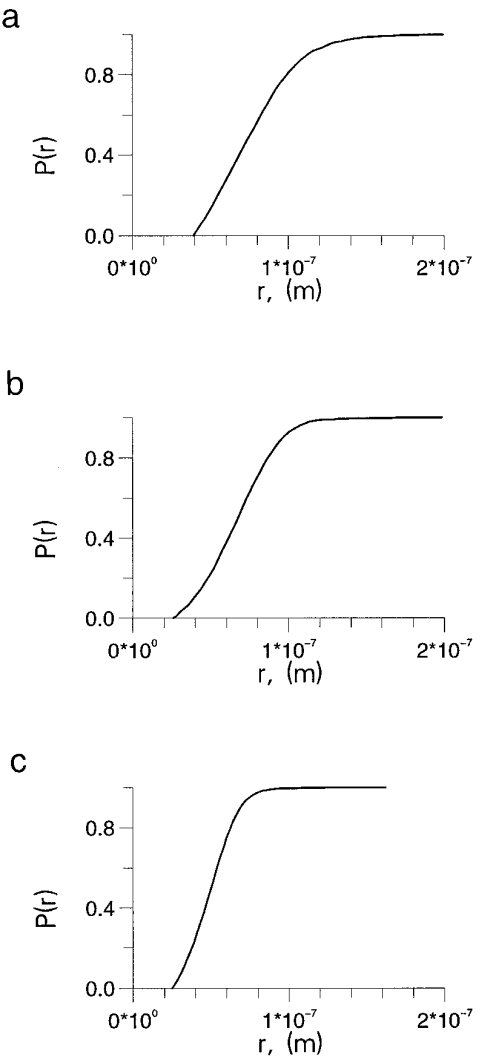

FIG. 7. Empirical cumulative profile size distribution function for the blends B075 (a), B075CM05 (b), B075CM10 (c), B075CM15 (d), and B075CM20 (e).

considerably. The results demonstrate clearly that the new method is a valuable tool for the analysis of such data.

6. CONCLUSIONS

In this contribution, a method for unfolding sphere size distributions given a sample of profile radii has been proposed which combines the advantages of kernel estimators with those of regularization methods. The essential concept of this method consists in the calculation of the empirical cumulative distribution function of the profile radii and the determination of the corresponding sphere size distribution with Tikhonov regularization. The method leads to a nonnegative and properly

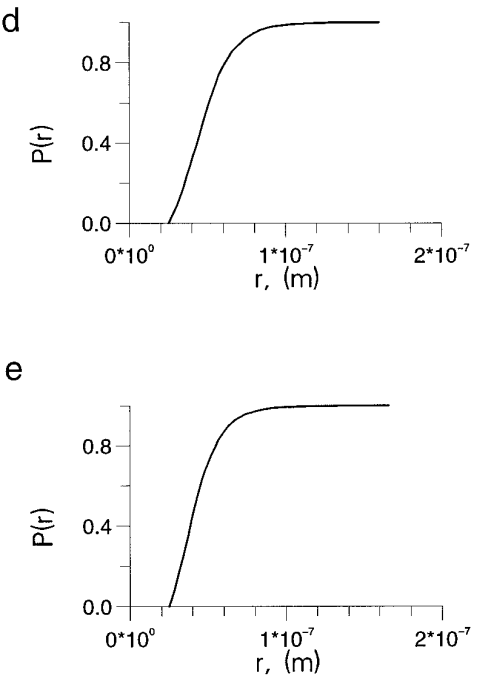

FIG. 7—*Continued*

normalized sphere size distribution. In addition, the method allows for automatically estimating the regularization parameter with the SC-method.

Using Monte-Carlo simulations it has been demonstrated that the method is reliable and leads to properly unfolded sphere size distributions. In particular, these simulations show that good values for the regularization parameter are obtained with the SC-method. Finally, the sphere size distributions of several polymer blends have been unfolded from TEM data. The application to experimental data confirms the excellent results of the Monte-Carlo simulations and demonstrates that the new method is a valuable tool for data analysis.

Within the method presented, the integral equation relating the cumulative profile size distribution function to the sphere size distribution can be replaced by any other linear integral equation. Similar to the smoothed EM-approach described in [34], the method may, therefore, also be applied to similar problems as, e.g., image reconstruction in emission tomography. It is an interesting question to be studied in the future whether such problems can also be solved with the method presented.

APPENDIX

For the numerical computations the functions and operators must be represented by finite-dimensional quantities. This can be done by approximating the integrals and derivatives by sums and difference coefficients. A simple approximation with a low degree of convergence is sufficient, because the approximation error is small, compared to the error caused by the regularization or the sample statistics.

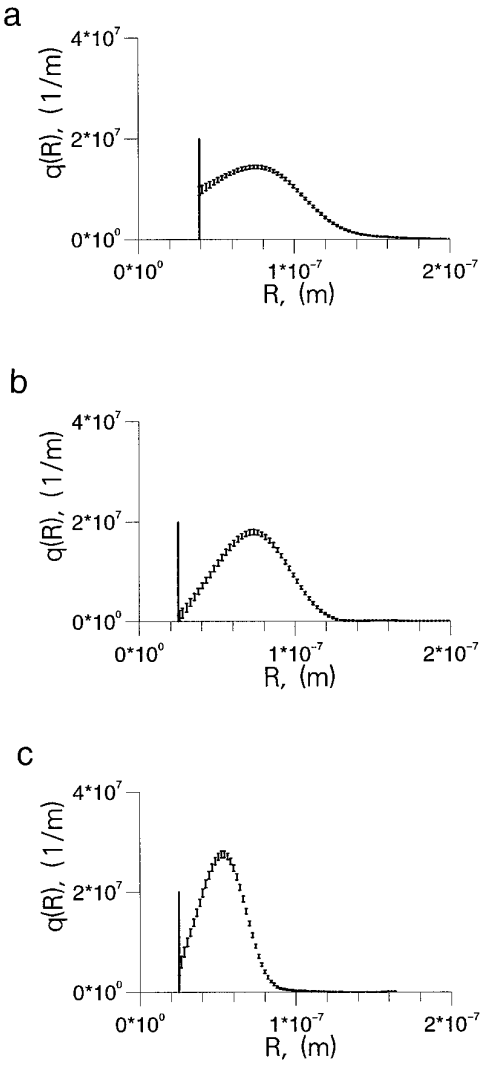

FIG. 8. Sphere size distribution for the blends B075 (a), B075CM05 (b), B075CM10 (c), B075CM15 (d), and B075CM20 (e). The straight line marks the resolution limit ε.

With such an approximation the scaled sphere size distribution $h(R)$ is given by the β coefficients $h_1, ..., h_\beta$:

$$h_j = h(R_j), \qquad j = 1, ..., \beta, \tag{27}$$

$$R_j = \varepsilon + (j-1)\Delta_R, \quad j = 1, ..., \beta, \tag{28}$$

$$\Delta_R = \frac{R_{\max} - \varepsilon}{\beta - 1}. \tag{29}$$

Using these coefficients $(Kh)(r)$ can be approximated according to

$$(Kh)(r) = \sum_{j=1}^{\beta} K_j(r) h_j \tag{30}$$

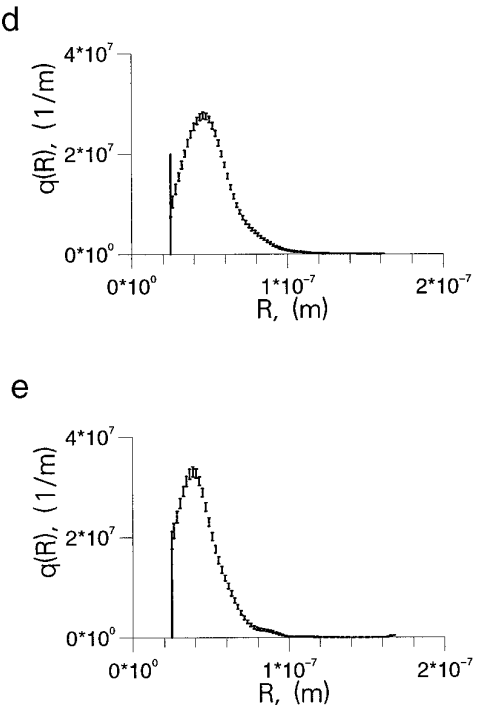

FIG. 8—*Continued*

with

$$K_j(r) = \begin{cases} 2\Delta_R \left(\dfrac{d}{2} + \sqrt{R_j^2 - r^2} \right), & r \le R_j, \\ 0, & r > R_j. \end{cases} \tag{31}$$

If the profile size distribution $p(r) = (Kh)'(r)$ is needed, there arise, however, difficulties, because the derivative of $K_j(r)$ does not exist at $r = R_j$. These difficulties

TABLE II
Number of Profiles and Resolution Limit Used to Obtain the Sphere Size Distributions Shown in Fig. 8

Blend	Number of profiles n	Resolution limit ε, (nm)	Regularization parameter λ
B075	4104	39.0	2.73×10^{-13}
B075CM05	2311	26.0	1.09×10^{-13}
B075CM10	3557	25.0	3.19×10^{-15}
B075CM15	4270	25.0	1.94×10^{-15}
B075CM20	3517	25.0	3.47×10^{-16}

Note. The value estimated with the SC-method for the regularization parameters λ is also listed.

can be avoided by assuming linear interpolation in the intervals between two successive coefficients h_j,

$$h(R) = \sum_{j=1}^{\beta} h_j \varphi_j(R) \tag{32}$$

with

$$\begin{aligned}
\varphi_1(R) &= \Delta_R^{-1} \begin{cases} (R_2 - R), & \varepsilon \le R \le R_2, \\ 0, & R_2 < R \le R_{\max}; \end{cases} \\
\varphi_j(R) &= \Delta_R^{-1} \begin{cases} 0, & \varepsilon \le R < R_{j-1} \\ (R - R_{j-1}), & R_{j-1} \le R < R_j \\ (R_{j+1} - R), & R_j \le R \le R_{j+1} \\ 0, & R_{j+1} < R \le R_{\max} \end{cases}, \quad j = 2, ..., \beta - 1; \\
\varphi_\beta(R) &= \Delta_R^{-1} \begin{cases} 0, & \varepsilon \le R < R_{\beta-1}, \\ (R - R_{\beta-1}), & R_{\beta-1} \le R \le R_{\max}. \end{cases}
\end{aligned} \tag{33}$$

Evaluating $K_j(r) = (K\varphi_j)(r)$, the expressions

$$\begin{aligned}
K_1(r) &= \mathscr{T}(R_2, R_1, r) - \mathscr{T}(R_2, R_2, r) \\
K_j(r) &= \mathscr{T}(R_{j+1}, R_j, r) - \mathscr{T}(R_{j+1}, R_{j+1}, r) \\
&\quad + \mathscr{T}(R_{j-1}, R_j, r) - \mathscr{T}(R_{j-1}, R_{j-1}, r), \quad j = 2, ..., \beta - 1 \\
K_\beta(r) &= \mathscr{T}(R_{\beta-1}, R_\beta, r) - \mathscr{T}(R_{\beta-1}, R_{\beta-1}, r)
\end{aligned} \tag{34}$$

with

$$\mathscr{T}(\rho, R, r) = \Delta_R^{-1} \begin{cases} \dfrac{\rho}{2}(r^2 \ln(R + \sqrt{R^2 - r^2}) - R\sqrt{R^2 - r^2}) \\ \quad + \dfrac{d}{4}(R - \rho)^2 + \dfrac{1}{3}(R^2 - r^2)^{3/2}, & R > r, \\ \left(\dfrac{d}{4}(r - \rho)^2 + \dfrac{\rho}{2} r^2 \ln r\right), & R \le r, \end{cases} \tag{35}$$

are obtained in this case, and the profile size distribution $p(r) = (Kh)'(r)$ can be computed straightforwardly by differentiation.

Starting with these expressions, the quantity $V(\lambda)$ of Eq. (13) has been approximated by

$$V(\lambda) = \Delta_r(\boldsymbol{K}\mathbf{h} - \mathbf{I} + \hat{\mathbf{P}})^2 + \lambda \Delta_R(\boldsymbol{L}\mathbf{h})^2. \tag{36}$$

To obtain the first term, the integration associated with the norm $\|\cdot\|^2$ has been replaced by a sum. With

$$r_i = \varepsilon + (i-1)\Delta_r, \quad i = 1, ..., \alpha, \tag{37}$$

$$\Delta_r = \frac{R_{\max} - \varepsilon}{\alpha - 1} \tag{38}$$

the coefficients of the matrix $\boldsymbol{K}$, the vector $\mathbf{I}$, and the vector $\hat{\mathbf{P}}$ are given by

$$K_{ij} = K_j(r_i), \quad i = 1, ..., \alpha; j = 1, ..., \beta \tag{39}$$

$$I_i = 1, \qquad i = 1, ..., \alpha \tag{40}$$

$$\hat{P}_i = \hat{P}(r_i), \quad i = 1, ..., \alpha. \tag{41}$$

The second term has also been obtained using a sum, instead of the integration associated with the norm $\|\cdot\|^2$. In addition the matrix $\boldsymbol{L}$ with coefficients

$$L_{ij} = \frac{1}{\Delta_R^2}(\delta_{ij} + \delta_{(i+2)j} - 2\delta_{(i+1)j}), \quad i = 1, ..., \beta - 2; j = 1, ..., \beta, \tag{42}$$

has been introduced as a discrete approximation of the second derivative represented by the operator L in Eq. (13).

Given the expression (36) for $V(\lambda)$, computation of the scaled sphere size distribution for a given value of the regularization parameter poses no problem. If no constraints must be taken into account, the normal equations associated with minimization of $V(\lambda)$ lead to

$$\hat{\mathbf{h}}_\lambda = \boldsymbol{K}^{-1}(\lambda)(\mathbf{I} - \hat{\mathbf{P}}) \tag{43}$$

with

$$\boldsymbol{K}^{-1}(\lambda) = \left(\boldsymbol{K}^t\boldsymbol{K} + \frac{\Delta_R}{\Delta_r}\lambda \boldsymbol{L}^t\boldsymbol{L}\right)^{-1} \boldsymbol{K}^t. \tag{44}$$

Positivity and proper normalization can be introduced by performing minimization of $V(\lambda)$, subject to the constraints

$$\sum_{j=1}^{\beta} K_{1j} h_j = 1 \tag{45}$$

$$h_j \geq 0, \quad j = 1, ..., \beta. \tag{46}$$

This quadratic optimization problem can be solved with a QP-algorithm [35] which can be found in well-known numeric libraries.

In order to estimate the regularization parameter defined by the SC-method, Eq. (22) has been solved with a standard algorithm for finding roots. Within the optimization, the quantity has been evaluated using the approximations introduced above:

$$\begin{aligned} ED_h(\hat{\mathbf{h}}_\lambda, \mu, n) = {} & \Delta_R(\hat{\mathbf{h}}_\lambda - \boldsymbol{K}^{-1}(\mu)(\mathbf{I} - \boldsymbol{K}\hat{\mathbf{h}}_\lambda))^2 \\ & + \frac{\Delta_r \Delta_R}{n} \sum_{i=1}^{\alpha} (\boldsymbol{K}^{-1}(\mu)\boldsymbol{\theta}_i)^2 (\boldsymbol{K}'\hat{\mathbf{h}}_\lambda)_i \\ & - \frac{\Delta_R}{n} (\boldsymbol{K}^{-1}(\mu)(\mathbf{I} - \boldsymbol{K}\hat{\mathbf{h}}_\lambda))^2. \end{aligned} \tag{47}$$

The vector $\boldsymbol{\theta}_i$ and the matrix $\boldsymbol{K}'$ are given by

$$\theta_{ij} = \begin{Bmatrix} 1, & R_j \geq r_i \\ 0, & R_j < r_i \end{Bmatrix}, \quad i = 1, ..., \alpha; j = 1, ..., \beta, \tag{48}$$

$$K'_{ij} = K'_j(r_i), \quad i = 1, ..., \alpha; j = 1, ..., \beta. \tag{49}$$

The other quantities have been defined above. It should be noted that the estimation of the regularization parameter is rather time consuming if $\boldsymbol{K}^{-1}(\lambda)$ is calculated by a matrix inversion in each iteration. Using the matrix decomposition described in [36] which is a kind of generalized singular decomposition, the computations are less consuming, because the matrix $\boldsymbol{K}^{-1}(\lambda)$ can be evaluated for different values of the regularization parameter without further matrix inversions.

Neglecting the constraints (45) and (46), the expression

$$\begin{aligned} \sigma^2(R_j) = {} & \frac{\Delta r}{n} \sum_{i=1}^{\alpha} (\boldsymbol{K}^{-1}(\lambda)\boldsymbol{\theta}_i)_j^2 (\boldsymbol{K}'\hat{\mathbf{h}}_\lambda)_i \\ & - \frac{1}{n} (\boldsymbol{K}^{-1}(\mu)(\mathbf{I} - \boldsymbol{K}\hat{\mathbf{h}}_\lambda))_j^2 \end{aligned} \tag{50}$$

is obtained for the variances $\sigma^2(R_j)$ (compare Eq. (25)). The positivity constraints have, however, a large influence on the unfolded scaled sphere size distribution $\hat{\mathbf{h}}_\lambda$ and on the corresponding variances $\sigma^2(R_1), ..., \sigma^2(R_\beta)$. This influence is represented by the set $\mathcal{M}$ of active constraints ($h_j = 0$ for $j \in \mathcal{M}$) obtained after minimization of $V(\lambda)$ with respect to the constraints (45) and (46). This set has been taken into account when computing the variances $\sigma^2(R_j)$; for $j \in \mathcal{M}$ the variances $\sigma^2(R_j)$ were assumed to be zero. To compute the other variances, the columns of the matrices $\boldsymbol{K}$ and $\boldsymbol{L}$ belonging to an active constraint have been removed, and the variances $\sigma^2(R_j)$ for $j \notin \mathcal{M}$ were computed according to Eq. (50) using the modified matrices.

ACKNOWLEDGMENTS

We thank Chr. Friedrich and R. Riemann for making the TEM data available.

REFERENCES

1. S. D. Wicksell, *Biometrika* **17,** 84 (1925).
2. E. B. Jensen and H. J. G. Gundersen, *Acta Stereologica* **6** (Suppl. II), 105 (1987).
3. J. Moeller, *J. Appl. Probab.* **25,** 322 (1988).
4. Chr. Friedrich, W. Gleinser, E. Korat, D. Maier, and J. Weese, *J. Rheol.* **39**(6), 1411 (1995).
5. A. M. Donald and E. J. Kramer, *J. Appl. Polym. Sci.* **27,** 3729 (1982).
6. S. Y. Hobbs, *Polym. Eng. Sci.* **26,** 74 (1986).
7. G. Cigna, P. Lomellini, and M. Merlotti, *J. Appl. Polym. Sci.* **37,** 1527 (1989).
8. R. A. Hall, *J. Mater. Sci.* **27,** 6029 (1992).
9. S. J. Choi and W. R. Schowalter, *Phys. Fluids* **18,** 420 (1975).
10. J. F. Palierne, *Rheol. Acta* **29,** 204 (1990).
11. D. Graebling, R. Muller, and J. F. Palierne, *Macromolecules* **26,** 320 (1990).
12. B. W. Silverman, *Density Estimations for Statistics and Data Analysis* (Chapman & Hall, London, 1986).
13. C. C. Taylor, *J. Microsc.* **132,** 57 (1983).
14. P. Hall and R. L. Smith, *J. Comput. Phys.* **74,** 409 (1988).
15. B. van Es and A. Hoogendoorn, *Biometrika* **77,** 139 (1990).
16. V. A. Morozov, *Methods for Solving Incorrectly Posed Problems* (Springer-Verlag, New York, 1984).
17. K. Kanatani and O. Ishikawa, *J. Comput. Phys.* **57,** 229 (1985).
18. H. W. Engl, *Surv. Math. Indus.* **3,** 71 (1993).
19. D. Nychka, G. Whaba, S. Goldfarb, and T. Pugh, *J. Am. Statist. Assoc.* **79,** 832 (1984).
20. W. Gleinser, D. Maier, M. Schneider, J. Weese, Chr. Friedrich, and J. Honerkamp, *J. Appl. Polym. Sci.* **53,** 39 (1994).
21. G. Bach, *Z. Wiss. Mikrok.* **64,** 265 (1959).
22. R. Coleman, *Biom. J.* **24** (3), 273 (1982).
23. L. M. C. Orive, *J. Micros.* **107,** 235 (1976).
24. R. S. Anderssen and F. R. de Hoog, *Numerical Solution of Integral Equations,* edited by M. A. Goldberg (Plenum, New York, 1990), p. 373.
25. L. M. C. Orive, *J. Micros.* **131,** 265 (1983).
26. J. Honerkamp and J. Weese, *Cont. Mech. Therm.* **2,** 17 (1990).
27. C. Eiche, D. Maier, M. Schneider, D. Sinerius, J. Weese, K. W. Benz, and J. Honerkamp, *J. Phys.: Cond. Matter* **4,** 6131 (1992).
28. J. Honerkamp, D. Maier, and J. Weese, *J. Chem. Phys.* **98**(2), 865 (1993).
29. J. Honerkamp and J. Weese, *Rheol. Acta* **32,** 65 (1993).
30. H. Schäfer, Ph.D. thesis, Universität Leipzig, 1994.
31. D. Maier, P. Hug, M. Fiederle, C. Eiche, D. Ebling, and J. Weese, *J. Appl. Phys.* **77**(8), 3851 (1995).
32. J. Weese, J. Hendricks, R. Zorn, J. Honerkamp, and D. Richter, *Nucl. Inst. Meth. A* **378,** 275 (1996).
33. R. Coleman, *J. Microscopy* **153,** 233 (1989).
34. B. W. Silverman, M. C. Jones, D. W. Nychka, and J. D. Wilson, *J. R. Statist. Soc. B* **52,** 271 (1990).
35. J. Stoer, *SIAM J. Numer. Anal.* **13,** 382 (1971).
36. J. Weese, *Comput. Phys. Commun.* **69,** 99 (1992).